NMR Spin Dynamics in Solids. I. Artificial Line Narrowing and Zeeman Spin-Spin Relaxation in the Rotating Frame*

P. MANSFIELD AND D. WARE
Department of Physics, University of Nottingham, Nottingham, England
(Received 5 September 1967)

An experimental and theoretical study is made of the response of a single-magnetic-species spin system to a coherent train of resonant 90° rf pulses of spacing 2τ, following at time τ an initial preparatory 90° pulse. The rf phase of the coherent pulses is shifted 90° with respect to the initial pulse. It is shown that this pulse sequence will produce a sustained "solid-echo" chain for times much greater than T_2, i.e., approaching the spin-lattice relaxation time. This therefore shows promise as a new method of chemical-shift measurement in solids, as well as a direct method of measuring the rotating-frame spin-lattice relaxation time $T_{1\rho}$. Except for a small initial oscillation, the amplitudes of successive even or odd echo maxima in CaF_2 are found to decay exponentially with a time constant $T_{2\epsilon}$. It is shown theoretically that a simple diagonal assumption for the density matrix plus the rotational symmetry properties of the dipolar Hamiltonian to 90° pulses could explain the observed τ^{-5} dependence of $T_{2\epsilon}$ as well as the oscillatory effect. Numerical evaluation of the magnitude of $T_{2\epsilon}$ based on a cumulant-moment approximation gives good agreement with experiment.

Further related experiments have been performed by spin-locking the F^{19} magnetization in long pulses of low amplitude. These experiments are intended to simulate the multiple-pulse sequences by replacing the coherent-pulse train with its mean field. The results reveal considerable oscillatory effects due to mutual exchange of energy between the Zeeman and dipolar subsystems in the rotating reference frame. A theoretical analysis is given which supports these effects. An estimate is made of the Zeeman dipolar cross-relaxation time, and is compared with Provotorov's theory as modified by Walstedt.

In the multiple-pulse experiment, the "solid-echo" amplitude modulation may be ascribed to mutual energy exchange between the rf Zeeman energy in the zeroth Fourier harmonic of the pulse train (the mean pulse field) and the dipolar energy. Because of the higher harmonics in the Fourier expansion, however, the initial oscillatory effects disappear as τ increases.

I. INTRODUCTION

WHEN solid materials containing nuclear spins in a high static magnetic field are irradiated with two or three short 90° rf pulses within a time of the order of T_2 and at the Larmor frequency, the system gives rise to a number of transient effects. With one spin species, a solid echo[1,2] arises from a $90°-\tau-90°_{90°}$ pulse sequence, where the subscript 90° refers to the relative rf phase of the pulses and τ is the pulse spacing. This case as well as other pulse sequences for one or two magnetic ingredients has been studied theoretically by Mansfield,[3] and a recent experimental study on solid Xenon has also been made by Warren and Norberg.[4]

In this paper, we present an experimental and theoretical study of the spin system when further $90°_{90°}$ pulses uniformly spaced at 2τ are applied to it in a continuous train. The effect of the pulses is to produce a continuous chain of solid echoes, thus prolonging the transverse decay by many orders of magnitude.[5] Similar experiments have been independently reported by Ostroff and Waugh.[6] Successive solid-echo peaks are found to decay exponentially with time constant $T_{2\epsilon}$, except for the first few echoes. These oscillate in amplitude slightly, the effect being readily observable for systems with two abundant magnetic ingredients. In our letter,[5] we showed that a naïve assumption regarding the progressive attenuation of the density matrix, based on the reduction of the first solid-echo amplitude, gives a τ^{-3} dependence of $T_{2\epsilon}$, which clearly does *not* fit our experimental data.

In the present work we show theoretically that a simple diagonal assumption for the density matrix for the even echoes, based on the rotational symmetry properties of the dipolar Hamiltonian to 90° pulses, explains the observed τ^{-5} dependence of $T_{2\epsilon}$ as well as the oscillatory effect. Approximate numerical evaluation of the constants involved gives remarkable agreement with experiment for the predicted magnitude of $T_{2\epsilon}$. A similar theory without numerical evaluation is given by Waugh and Wang[7] based on the binomial decay approximation.[5]

Our experiments correspond to a narrowing of the resonance absorption line shape plus the introduction of sidebands. Viewed this way, they show promise as a new method of chemical shift measurement in solids. To this extent, the experiments here resemble other line-narrowing experiments,[8–10] in which the sample inclined to $\mathbf{H}_0$ at the magic angle is physically rotated. The criterion for significant line narrowing is similar in both cases.

* Work supported by an equipment grant from the Science Research Council.

[1] J. G. Powles and P. Mansfield, Phys. Letters **2**, 58 (1962); I. J. Lowe, Bull. Am. Phys. Soc. **2**, 344 (1957).
[2] J. G. Powles and J. H. Strange, Proc. Phys. Soc. (London) **82**, 6 (1963).
[3] P. Mansfield, Phys. Rev. **137**, A961 (1965).
[4] W. W. Warren and R. E. Norberg, Phys. Rev. **154**, 277 (1967).
[5] P. Mansfield and D. Ware, Phys. Letters **22**, 133 (1966).
[6] E. D. Ostroff and J. S. Waugh, Phys. Rev. Letters **16**, 1097 (1966).
[7] J. S. Waugh and C. H. Wang, Phys. Rev. **162**, 209 (1967).
[8] E. R. Andrew, A. Bradbury, and R. G. Eades, Arch. Sci. (Geneva) **11**, 223 (1958).
[9] I. J. Lowe, Phys. Rev. Letters **2**, 285 (1959).
[10] J. Dreitlein and H. Kessemeier, Phys. Rev. **123**, 835 (1961).

We have reported preliminary experiments in which such pulse sequences are applied to the sodium resonance in a single crystal of NaF.[11] In this case it is possible to perform double resonance experiments analogous to those of Hartmann and Hahn[12] and Lurie and Slichter.[13] Preliminary experiments have also been carried out on Al^{27} in metallic aluminium.[14] In this case, T_1 is quite short, thereby affording a test of the applicability of multiple-pulse solid-echo trains to the direct measurement of spin-lattice interactions in the rotating frame. In the present work, however, we restrict ourselves to a discussion of single spin ingredient systems, and to the dipolar spin-spin interaction only. Full discussion of two magnetic species systems and the introduction of a spin-lattice interaction and particularly the chemical shift will be presented later.

We also present a theoretical and experimental study of some related experiments in which the spin magnetization following a short 90° pulse is "spin locked" in a long low-power rf pulse at resonance. The magnetization is inspected by observing the free induction decay following rapid turnoff of the pulse. It is found to be a damped oscillating function of time decaying through a quasiequilibrium state to a final steady value. Both the periodicity and final value of the magnetization are functions of the spin-locking field. These experiments are analogous to the laboratory-frame experiments of Strombotne and Hahn.[15] They differ in that their system was prepared initially in an adiabatically demagnetized state. Calculations related to these experiments have been made by Jeener, Eisendrath, and Van Steenwinkel,[16] and show that the rf field can cause the magnetic energy of the spin system to oscillate back and forth between the Zeeman and dipolar reservoirs in times of the order of T_2. In a further paper,[17] Jeener, du Bois, and Broekaert have shown experimentally that the exact analog of the Strombotne and Hahn experiments, i.e., adiabatic demagnetization in the rotating frame followed by a long rf pulse does produce an oscillation of the dipolar order. A further experiment, concerned with the growth of magnetization from the demagnetized state, has been reported by Einbinder and Hartmann.[18]

Phenomenologically, the oscillations may be ascribed to classical precession of the spins about a distribution of effective fields. These are made time-dependent by the local fields due to the spin-flip terms in the dipolar Hamiltonian. By considering the rf pulse train in the previous experiments as principally a mean continuous rf field, which is true for close pulse spacing, we see physically that the origin of the initial solid-echo amplitude oscillations is the same. The disappearance of the oscillation corresponds to an attempt at establishment of a Zeeman spin temperature.

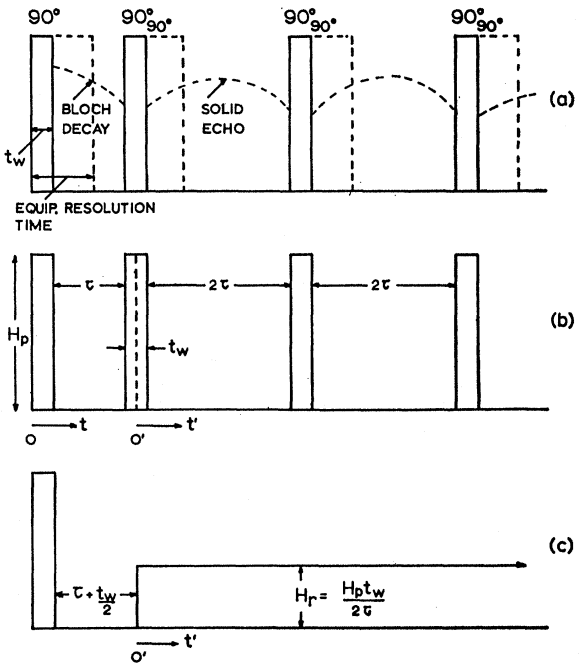

FIG. 1. (a) Sketch of the modulus of a

$$90°-\tau-90°_{90°}-(2\tau-90°_{90°})_{N-1}$$

rf pulse-train envelope. The dotted curve indicates the formation of successive solid echoes outside the equipment resolution time. (b) Pulse sequence as in (a) above. (c) First approximation to pulse sequence (b). The coherent phase-shifted pulse train is replaced by its zero-frequency Fourier component.

A further small decrease in the spin-locked magnetization for long pulses has been observed. This corresponds to an energy conserving cross-relaxation between the Zeeman and dipolar energy reservoirs. From these experiments we estimate the cross-relaxation time and compare this with Walstedt's[19] theoretical expression.

II. THEORY

A. Multiple-Pulse Analysis

We wish to calculate the transverse response when a $90°-\tau-90°_{90°}-(2\tau-90°_{90°})_{N-1}$ rf pulse sequence is applied at resonance to a single-species spin system of spin I initially in thermal equilibrium in a large static magnetic field $\mathbf{H}_0$. Here N denotes the total number of

[11] P. Mansfield and D. Ware, Phys. Letters **23**, 421 (1966).
[12] S. R. Hartmann and E. L. Hahn, Phys. Rev. **128**, 2042 (1962).
[13] F. M. Lurie and C. P. Slichter, Phys. Rev. **133**, A1108 (1964).
[14] P. Mansfield and D. Ware, in *Proceedings of the Fourteenth Colloque Ampère (Atomes et Molécules par des Etudes Radio-Electriques) 1962* (North-Holland Publishing Co., Amsterdam, 1966).
[15] R. L. Strombotne and E. L. Hahn, Phys. Rev. **133**, A1616 (1964).
[16] J. Jeener, H. Eisendrath, and R. Van Steenwinkel, Phys. Rev. **133**, A478 (1964).
[17] J. Jeener, R. DuBois, and P. Broekaert, Phys. Rev. **139**, A1959 (1965).
[18] H. M. Einbinder and S. R. Hartmann, Phys. Rev. Letters **17**, 518 (1966).
[19] R. E. Walstedt, Phys. Rev. **138**, A1096 (1965).

coherent 90° rf pulses; the subscript 90° means the phase is in quadrature with the initial rf pulse, and τ is the time between pulses. This sequence is represented in Fig. 1(a).

Between rf pulses, the spin Hamiltonian is

$$\hbar\mathcal{H}=(\mathcal{H}_0+\sum_{\pm M}\mathcal{H}_1{}^M+\mathcal{H}_{SL})\hbar, \tag{1}$$

where $\mathcal{H}_0$ is the Zeeman part, $\hbar\mathcal{H}_{SL}$ is the spin-lattice interaction Hamiltonian, and $\hbar\sum_{\pm M}\mathcal{H}_1{}^M$ is the total rigid-lattice dipolar interaction. In fact, we are interested only in the truncated dipolar term[20] $\mathcal{H}_1{}^0$ in the laboratory reference frame, so in this section we may take the superscript, zero as understood, i.e.,

$$\mathcal{H}_1{}^0=\mathcal{H}_1=\sum_{k>j}(A_{jk}+\tilde{A}_{jk})\mathbf{I}_j\cdot\mathbf{I}_k+B_{jk}I_{z_j}I_{z_k}, \tag{2}$$

where for a pair of spins jk of internuclear distance r_{jk}, and with the vector $\mathbf{r}_{jk}$ making an angle θ_{jk} with $\mathbf{H}_0$

$$A_{jk}=-\tfrac{1}{2}\gamma^2\hbar(1-3\cos^2\theta_{jk})/r_{jk}{}^3,$$
$$B_{jk}=\tfrac{3}{2}\gamma^2\hbar(1-3\cos^2\theta_{jk})/r_{jk}{}^3.$$

$\tilde{A}_{jk}$ is the exchange-interaction coupling constant. If the rf-pulse Hamiltonian $\hbar\mathcal{H}_p\gg\hbar\mathcal{H}_1$, the rf pulses can be treated as rotation operators. In this case, the initial 90° pulse can be represented by a transformation operator $R_0=\exp(i\pi I_y/2)$, i.e., a rotation about the y axis in the frame of reference rotating at the Larmor angular frequency ω_0. The subsequent 90° pulses are rotations about the x axis and are all represented by rotation operators $R_N=\exp(i\pi I_x/2)$. The case for $N=1$ has been previously calculated,[2,3] and gives for the transverse magnetization at time $t=\tau+t'$

$$\langle I_x\rangle=(\cos\omega_0 t/\mathrm{Tr}\{I_x{}^2\})\ \mathrm{Tr}\{\exp(-i\mathcal{H}_1t')\times R_1{}^\dagger\exp(-i\mathcal{H}_1\tau)R_0{}^\dagger\rho(0)R_0\times\exp(i\mathcal{H}_1\tau)R_1\exp(i\mathcal{H}_1t')I_x\}, \tag{3}$$

where

$$\rho(0)=\frac{\exp(-\hbar\mathcal{H}/kT)}{\mathrm{Tr}\{\exp(-\hbar\mathcal{H}/kT)\}}\simeq\hbar\omega_0I_z/kT\ \mathrm{Tr}\{1\}=aI_z$$

is the initial thermal-equilibrium density matrix, which is approximated for high temperature T. Here k is Boltzmann's constant. On expanding the exponential operators and evaluating the traces, Eq. (3) reduces to

$$\langle I_x\rangle=a\cos\omega_0t(1-M_2(\tau-t')^2/2!+M_4(\tau-t')^4/4!-\cdots+\tfrac{1}{4}M_{4\epsilon}\tau^2t'^2+\cdots). \tag{4}$$

M_2 and M_4 are the Van Vleck moments of the absorption line shape. When $t'=\tau$, this equation predicts a "solid echo," the maximum amplitude of which is reduced by the fourth-moment-like error term $M_{4\epsilon}$, where

$$M_{4\epsilon}=-M_4+M_{4x}, \tag{5a}$$

$$M_{4x}=\mathrm{Tr}\{[\mathcal{H}_1',[\mathcal{H}_1',I_x]][\mathcal{H}_1,[\mathcal{H}_1,I_x]]\}/\mathrm{Tr}\{I_x{}^2\}, \tag{5b}$$

and

$$\mathcal{H}_1'=R_1{}^\dagger\mathcal{H}_1R_1. \tag{5c}$$

Explicit calculation of $M_{4\epsilon}$ for any spin I is given in Ref. 3. The above expressions are easily extended for any N, in which case restricting ourselves to a description of the echo maxima, i.e., $t'=\tau$, we get, for $N>0$ and even,

$$\langle I_x(2N\tau)\rangle=(a\cos\omega_0t/\mathrm{Tr}\{I_x{}^2\})\ \mathrm{Tr}\{\rho(2N\tau)I_x\}, \tag{6a}$$

where

$$\rho(2N\tau)=\exp(-i\mathcal{H}_1\tau)\ \exp(-i\mathcal{H}_1'2\tau)O^{\dagger n}\times\exp(-i\mathcal{H}_1\tau)I_x\exp(i\mathcal{H}_1\tau)O^n\exp(i\mathcal{H}_1'2\tau)\ \exp(i\mathcal{H}_1\tau) \tag{6b}$$

and

$$n=(N-2)/2. \tag{6c}$$

The symmetry of the dipolar interaction under 90° rotations permits a pairing of the exponential terms to form the operator

$$O=\exp(i\mathcal{H}_1'2\tau)\ \exp(i\mathcal{H}_1 2\tau).$$

Thus Eq. (6a) may be written in terms of the new discrete variable Eq. (6c), giving

$$\langle I_x[(n+1)4\tau]\rangle=(a\cos\omega_0t/\mathrm{Tr}\{I_x{}^2\})\times\mathrm{Tr}\{\rho[(n+1)4\tau]I_x\}. \tag{6d}$$

In the case of $N>0$ and odd, the density matrix in Eq. (6a) becomes

$$\rho(2N\tau)=\exp(-i\mathcal{H}_1\tau)\tilde{O}^{\dagger n}\exp(-i\mathcal{H}_1'\tau)I_x\times\exp(i\mathcal{H}_1'\tau)\tilde{O}^n\exp(i\mathcal{H}_1\tau), \tag{6e}$$

where now

$$n=(N-1)/2 \tag{6f}$$

and

$$\tilde{O}=\exp(i\mathcal{H}_1 2\tau)\ \exp(i\mathcal{H}_1'2\tau).$$

We wish to calculate the decay time constant of the train of even echo maxima. Except for an initial transient which we discuss in detail later, experiment indicates that successive echo maxima decay exponentially in all cases. Rather than attempt the formidable task of expanding and evaluating Eq. (6d) directly to give the envelope of successive echo maxima, we propose to evaluate the logarithmic decre-

[20] J. H. Van Vleck, Phys. Rev. **74**, 1168 (1948).

ment for an exponential decay and in this way obtain an expression for the effective relaxation time $T_{2\epsilon}$ of the solid echo train. In general, if the logarithmic decrement is independent of n, then Eq. (6d) is truly exponential. Thus we wish to evaluate the quotient

$$\langle I_x[(n+2)4\tau]\rangle/\langle I_x[(n+1)4\tau]\rangle=\langle I_x(t+4\tau)\rangle/\langle I_x(t)\rangle, \tag{7}$$

where we note that the total time to the Nth echo maximum is $t=(n+1)4\tau$. The rigorous procedure would be to substitute Eqs. (6b) and (6d) into Eq. (7), expand the numerator and the inverse denominator as a power series in n, then sum all terms independent of n. This method would doubtless select the main exponential terms and hence evaluate the time constant. We choose to avoid expansion by making a simple assumption regarding the diagonality of the density matrix $\rho(t)$. As we shall see, this is similar to our previous assumption,[5] but now takes account of the rotational symmetry of the dipolar interaction. Since we are dealing specifically with the even echo maxima, our assumption ignores periodic time dependencies, which give rise to cusps in the transverse decay or side bands in the Fourier transform.

1. Diagonal Assumption

We introduce a projection operator P such that $P\rho(t)$ selects the diagonal part of the density matrix in a representation in which I_x is diagonal. That is to say, we view the spins as being partially locked in the direction of the mean rf field along the x axis in the rotating reference frame. Thus we write

$$\rho(t)=P\rho(t)+(1-P)\rho(t). \tag{8}$$

The diagonal assumption puts $(1-P)\rho(t)=0$. This is clearly not always zero from the results in Ref. 5, and also from Sec. IIB for the truly spin-locked case (discussed below). There we show that initial transients are set up corresponding to an oscillatory spin-locked signal. The density matrix is clearly most diagonal when the Zeeman signal is a maximum and least diagonal at the signal minima. We have an analogous situation here. From the rotational symmetry of the dipolar Hamiltonian to 90° pulses we see that an even number of pulses recovers the original Hamiltonian i.e. $R^{\dagger N}\mathcal{H}_1R^N=\mathcal{H}_1$ for N even. The *actual* time between echo maxima in this case is 4τ, which, for a single-spin species system, corresponds precisely to a precessional period of the spins at twice the Larmor frequency in a mean pulse field, i.e., $4\tau=\pi/\gamma\bar{H}_p$. We propose, therefore, that an initially diagonal density matrix is in its most diagonal state after an even number of pulses. Introducing a function

$$f(N)=0, \quad N \text{ even}$$
$$=1, \quad N \text{ odd}$$

we modify Eq. (8) to

$$\rho(t)=P\rho(t)+(1-P)f(N)\rho(t). \tag{9}$$

Evaluating the quotient Eq. (7) using Eq. (9), we obtain for even N

$$\frac{\langle I_x(t+4\tau)\rangle}{\langle I_x(t)\rangle}=\frac{\mathrm{Tr}\{\exp(-i\mathcal{H}_1\tau)\exp(-i\mathcal{H}_1'2\tau)\exp(-i\mathcal{H}_1\tau)P\rho(t)\exp(i\mathcal{H}_1\tau)\exp(i\mathcal{H}_1'2\tau)\exp(i\mathcal{H}_1\tau)I_x\}}{\mathrm{Tr}\{P\rho(t)I_x\}}. \tag{10}$$

From the definition of the projection operator we note that $P\rho(t)=\alpha(t)I_x$, where $\alpha(t)$ is a time-dependent function, independent of the spin operators. Using this result and the definition of the logarithmic decrement we obtain finally for Eq. (10)

$$\exp(-4\tau/T_{2\epsilon})=\mathrm{Tr}\{\exp(-i\mathcal{H}_1\tau)\exp(-i\mathcal{H}_1'2\tau)\exp(-i\mathcal{H}_1\tau)I_x\exp(i\mathcal{H}_1\tau)\exp(i\mathcal{H}_1'2\tau)\exp(i\mathcal{H}_1\tau)I_x\}/\mathrm{Tr}\{I_x^2\}. \tag{11}$$

Successive even solid-echo peaks therefore follow the rate equation

$$d\langle I_x(t)\rangle/dt=-\langle I_x(t)\rangle/T_{2\epsilon}.$$

In this approximation, evaluation of $T_{2\epsilon}$ reduces to calculation of the error term for the second echo only, i.e., $N=2$ in Eqs. (6a)–(6c). As we shall see later in Sec. IIA3, the leading error term in the expansion of the right-hand side of Eq. (11) varies as τ^6, and its coefficient thus has the character of a sixth moment.

We have so far discussed only even echoes. From the properties of the density matrix Eq. (9), however, we have for odd N

$$\rho(2N\tau)=P\rho(2N\tau)+(1-P)\rho(2N\tau)$$
$$\equiv\exp(-i\mathcal{H}_1\tau)\exp(-i\mathcal{H}_1'\tau)P\rho[2(N-1)\tau]\exp(i\mathcal{H}_1'\tau)\exp(i\mathcal{H}_1\tau).$$

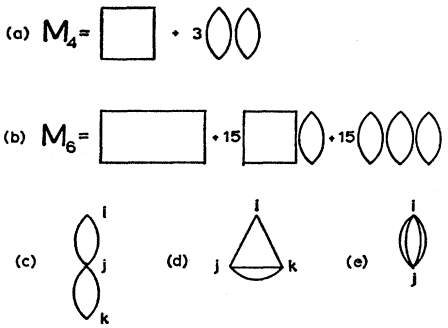

FIG. 2. Cumulant diagrams representing the fourth and sixth moments.

This allows us to take account of the nondiagonal character of the density matrix and thus enables us to calculate the logarithmic decrement between successive odd echoes.

Physically, the diagonal assumption implies that any loss of echo amplitude at the even echoes is completely irreversible. If this were true, another 90° pulse should produce an echo with a fourth-moment-like principal error term. This is discussed next for the particular case of three pulses.

2. *Third Echo at $t=6\tau$*

In this case $N=3$ in Eq. (6f). Expanding up to τ^4 only we find that

$$\langle I_x(6\tau)\rangle = a\cos\omega_0 t(1+\tfrac{1}{4}M_{4\epsilon}\tau^4+\cdots). \quad (12)$$

This result is similar to the first-echo case Eq. (4), and one would have to go to higher order in τ in both first- and third-echo expansions to discuss the differences. The alternate appearance of fourth-moment-like and sixth-moment-like principal error terms for odd and even echoes implies an oscillation of the echo maxima for short τ, the odd echoes being lower than the even echoes. The physical explanation of this oscillatory behavior is discussed in more detail in Sec. IIB, but we remark that for a single spin species, as discussed here, the periodicity is *twice* the pulse periodicity, i.e., 4τ. Thus the large echoes should occur after pairs of pulses, in spite of the fact that two 90° pulses constitute a step rotation of only 180°. As mentioned previously, this arises because of the symmetry of the dipolar interaction. We emphasize that this is *not* true for spin systems containing two magnetic ingredients, and in general four 90° pulses are required to recover $\mathcal{H}_1$. One would therefore expect transient oscillations with double the period, i.e., 8τ.

3. *Expansion of the Quotient*

We expand the right-hand side of Eq. (11) in a power series in time, including all powers up to τ^6. For this purpose, the numerator is rearranged as follows:

$$\mathrm{Tr}\{\exp(-i\mathcal{H}_1'\tau)I_x^\dagger(\tau)\exp(i\mathcal{H}_1'\tau)\exp(i\mathcal{H}_1'\tau)I_x(\tau)\times\exp(-i\mathcal{H}_1'\tau)\}, \quad (13a)$$

where

$$I_x(\tau)=\exp(i\mathcal{H}_1\tau)I_x\exp(-i\mathcal{H}_1\tau). \quad (13b)$$

To facilitate manipulation, we introduce the Liouville operators[21] L and L' defined by the relations

$$LI_x=[\mathcal{H}_1, I_x] \quad (14a)$$

and

$$L'I_x=[\mathcal{H}_1', I_x]. \quad (14b)$$

Expanding Eq. (13) and collecting coefficients of τ^m, we obtain for all terms up to $m=6$

$$\exp(-4\tau/T_{2\epsilon})=(1-M_{6\epsilon}\tau^6/18+\text{ higher-order terms}), \quad (15)$$

where

$$M_{6\epsilon}=\mathrm{Tr}\{-5(L^3I_x)(L^3I_x)+4(L^3I_x)(L'^3I_x)-12(L^4I_x)(L'^2I_x)-6(L^3I_x)(L'L^2I_x)-9(L'L^2I_x)(L'L^2I_x)\}/\mathrm{Tr}\{I_x^2\} \quad (16)$$

and is not in general equal to the sixth-moment error term for the first echo. If τ is small and $\tau/T_{2\epsilon}\ll 1$, we may expand the exponential in Eq. (15) and take $(M_{6\epsilon}/18)\tau^6$ to be the principal error term, yielding

$$T_{2\epsilon}=72/M_{6\epsilon}\tau^5. \quad (17)$$

The right-hand side of Eq. (15) is of course the normalized second-echo amplitude at $t=4\tau$. Unlike the first- and third-echo calculations, we note that the coefficient of τ^4 vanishes.[22]

4. *Approximate Evaluation of $M_{6\epsilon}$*

In order to evaluate the rather complex traces in Eq. (16), we adapt the method of cumulant averages to obtain an approximate expression. This method has been used by Horwitz and Callen[23] in ferromagnetic problems and is related to diagrammatic methods of lattice summation. The specific application of this method to the present problem is presented in Appendix A. As an example of the technique, the Van Vleck fourth moment can be related to products of lower nonzero moments plus a cumulant remainder, i.e.,

$$M_4=3M_2^2+K(L^4),$$

where $K(L^4)$ is the fourth-order cumulant remainder. This follows from Eq. (A9) plus the fact that there are no irreducible second-order cumulants. We can of course evaluate M_4 and related quantities exactly, but for higher moments, in particular M_6, exact evaluation is extremely tedious. In our approximation, we consistently discard all sixth-order cumulants, retaining all lower orders.

---

[21] The use of the Liouville operator and projection operator closely follows the methods of Provotorov (Ref. 25).

[22] This fact is pointed out by Ostroff and Waugh in Ref. 6.

[23] G. Horwitz and H. B. Callen, Phys. Rev. **124**, 1757 (1961).

We may represent the class of cumulants $K(L^n)$ by a connected diagram of n lines and n vertices. The fourth- and sixth-moment diagrams in this scheme are shown in Figs. 2(a) and 2(b). From Fig. 2(b) our sixth-moment approximation is therefore

$$M_6 \simeq 15M_4M_2 - 30M_2^3.$$

We point out that the vertex points in $K(L^4)$, Fig. 2(a) for example, do not necessarily represent different lattice sites. In this particular case, there are three distinct vertices i, j, k, so that this class breaks down into three four-line particle diagrams Figs. 2(c)–2(e).

Applying these ideas and Eqs. (A9)–(A11) and making the further approximation that the symmetrized averages may be replaced by normal averages, we obtain the approximate expressions for the traces appearing in Eq. (16):

$$\mathrm{Tr}\{(L^3I_x)(L^3I_x)\}/\mathrm{Tr}\{I_x^2\} = -15M_4M_2 + 30M_2^3, \quad (18a)$$

$$\mathrm{Tr}\{(L^3I_x)(L'^3I_x)\}/\mathrm{Tr}\{I_x^2\} = 9M_2M_{4x} + 6M_2M_4 - 30M_2^3, \quad (18b)$$

$$\mathrm{Tr}\{(L^4I_x)(L'^2I_x)\}/\mathrm{Tr}\{I_x^2\} = 9M_2M_4 + 6M_2M_{4x} - 30M_2^3, \quad (18c)$$

$$\mathrm{Tr}\{(L^3I_x)(L'L^2I_x)\}/\mathrm{Tr}\{I_x^2\} = 10M_2M_{4x} + 5M_2M_4 - 30M_2^3, \quad (18d)$$

$$\mathrm{Tr}\{(L'L^2I_x)(L'L^2I_x)\}/\mathrm{Tr}\{I_x^2\} = -5M_2M_4 - 10M_2M_{4x} + 30M_2^3. \quad (18e)$$

Substituting the above expressions into Eq. (16) and using Eq. (5a), we obtain finally the surprisingly simple result

$$M_{6\epsilon} \simeq -6M_2M_{4\epsilon}. \quad (19)$$

Substituting this into Eq. (17) gives us the central result of our calculation:

$$T_{2\epsilon} = -12/M_2M_{4\epsilon}\tau^5. \quad (20)$$

5. *Naïve Theory*

We include a brief discussion of our earlier elementary approach.[5] It was assumed that the density matrix describing the spin system at the first and subsequent echo maxima was in essentially the same state as after the initial 90° pulse, but slightly attenuated, i.e.,

$$\rho(2N\tau) = \rho(2[N-1]\tau)(1 + \tfrac{1}{4}M_{4\epsilon}\tau^4 + \cdots).$$

This follows from Eq. (4) evaluated at $t' = \tau$. Thus, after N coherent pulses, and taking $M_{4\epsilon}$ to be the principal error term, we get the binomial decay

$$\langle I_x \rangle = \langle I_x \rangle_0 (1-\epsilon\tau)^N,$$

where $\epsilon = -\frac{1}{4}M_{4\epsilon}\tau^3$. For $\epsilon\tau < 1$ and N large, the above expression may be approximated by $\langle I_x \rangle = \langle I_x \rangle_0 \exp(-\frac{1}{2}\epsilon t)$, where $t = 2N\tau$, yielding an effective transverse relaxation time $T_{2\epsilon} = -8/M_{4\epsilon}\tau^3$. As previously noted, this expression gives the wrong τ dependence for $T_{2\epsilon}$, though its magnitude will clearly straddle the experimental data.

We also note that even for small N, successive echoes give good exponential fit in CaF_2. Thus it seems more appropriate to assume an exponential decay directly rather than a binomial decay.

B. cw Spin Locking

It is clear from Fig. 1(b) that an alternative analysis of multiple-pulse trains can be made by considering the evolution of the spin system under the influence of the various cw Fourier components of the coherent-pulse train. Strictly speaking, this is true only if the various Fourier harmonics produce proportional changes in the density matrix, i.e., if the system is linear. (It is evident that very low intensity Fourier components will not produced linearly additive terms because of relaxation processes.) For simplicity, consider the Fourier transform of an infinite train of pulses of spacing 2τ and pulse width t_w. Let the origin of this sequence be O' with respect to the original pulse sequence [see Fig. 1(b)] since we are describing only the coherent pulses. The error in total time is small if we take $t = t' + \tau$, neglecting $t_w/2$. By doing this the Fourier transform is an even function about O'. Thus we may write the rf-field Hamiltonian applied at time τ as

$$\hbar\mathfrak{IC}_r(t') = (\hbar\mathfrak{IC}_p t_w/2\tau) + \sum_l \hbar\mathfrak{A}_l \cos(l\pi/\tau)t', \quad (21)$$

where

$$\mathfrak{A}_l = (\mathfrak{IC}_p t_w/\tau)(\sin\beta/\beta),$$

$$\beta = (l\pi t_w/2\tau) \qquad l = 1, 2, 3\cdots$$

From now on we take the primed time frame as understood. If the coherent pulses are applied at angular frequency ω along the x axis in the rotating frame, we have

$$\mathfrak{IC}_p = -\gamma H_p \exp(i\omega I_z t) I_x \exp(-i\omega I_z t).$$

Thus the equation of motion of a transformed density matrix

$$\rho^*(t) = \exp(-i\omega I_z t)\rho(t)\exp(i\omega I_z t)$$

under the influence of the total Hamiltonian $\hbar\mathfrak{IC} = \hbar(\mathfrak{IC}_0 + \mathfrak{IC}_1 + \mathfrak{IC}_r)$ is

$$d\rho^*(t)/dt = -i[-\Delta\omega I_z + \mathfrak{IC}_1 - \tilde{\omega}_r I_x - \sum_l \gamma A_l [\cos(l\pi/\tau)t] I_x, \rho^*], \quad (22)$$

where

$$\tilde{\omega}_r = \gamma\bar{H}_r = \gamma(H_p t_w/2\tau), \qquad \Delta\omega = \omega_0 - \omega$$

and

$$A_l = -\mathfrak{A}_l\hbar/\gamma I_x.$$

As in the previous section, we ignore the spin-lattice interaction. This is valid if the experiment is performed in a time less than $T_{1\rho}$. In the analysis which follows, we consider only the zeroth Fourier component or mean value of the rf pulse train. Thus we do *not* expect to predict by this method the details of solid-echo trains. This would clearly require including at least the first few Fourier harmonics. However, to the extent that the mean field is dominant in these experiments, i.e., for fairly close pulse spacing, we may expect to predict some of the characteristics of the spin magnetization. As we shall see, neglect of the harmonics predicts a constant spin-locked magnetization for large times. Following Redfield's ideas,[24] Eq. (22) may be written as

$$d\rho^*(t)/dt=-i[-\omega_{r\,\mathrm{eff}}\exp(-i\Theta I_y)I_z \times\exp(i\Theta I_y)+\mathcal{H}_1,\rho^*], \quad (23)$$

where

$$\omega_{r\,\mathrm{eff}}=\sqrt{(\Delta\omega^2+\bar{\omega}_r^2)},$$

and $\tan\Theta=\bar{\omega}_r/\Delta\omega$. I_z is the spin component along the new z axis of quantization which is the effective field vector in the tilted rotating frame. We transform the density matrix into this tilted frame by a time-independent unitary transformation:

$$S^\dagger(\Theta)\rho^*S(\Theta)=\rho^{*\prime}. \quad (24)$$

In the remainder of this section, we calculate all quantities in the tilted rotating frame, taking the asterisk and prime as understood. Thus Eq. (23) becomes

$$d\rho/dt=-i[-\omega_{r\,\mathrm{eff}}I_z+\sum_{M=-2}^{2}G_M,\rho], \quad (25)$$

where

$$S^\dagger\mathcal{H}_1S=G=\sum_{M=-2}^{2}G_M,$$

and

$$G_0=\sum_{k>j}A_{jk}'\mathbf{I}_j\cdot\mathbf{I}_k+B_{jk}'I_{zj}I_{zk},$$

$$G_{\pm1}=\sum_{k>j}E_{jk}'(I_{zk}I_{\pm j}+I_{zj}I_{\pm k}),$$

$$G_{\pm2}=\sum_{k>j}D_{jk}'I_{\pm j}I_{\pm k}.$$

The primed quantities are defined as follows:

$$A_{jk}'=\tilde{A}_{jk}+\tfrac{1}{2}A_{jk}(3\cos^2\Theta-1),$$

$$B_{jk}'=\tfrac{1}{2}B_{jk}(3\cos^2\Theta-1),$$

$$D_{jk}'=\tfrac{1}{4}(B_{jk}\sin^2\Theta),$$

$$E_{jk}'=-\tfrac{1}{2}(B_{jk}\sin\Theta\cos\Theta).$$

In order to integrate Eq. (25) we finally make a transformation to a reference frame rotating about the z axis, which then gives

$$d\hat{\rho}/dt=-i[\hat{G},\hat{\rho}], \quad (26)$$

where

$$\hat{G}=\exp(i\omega_{r\,\mathrm{eff}}I_zt)G\exp(-i\omega_{r\,\mathrm{eff}}I_zt)$$

and

$$\hat{\rho}=\exp(i\omega_{r\,\mathrm{eff}}I_zt)\rho\exp(-i\omega_{r\,\mathrm{eff}}I_zt).$$

A reiterative solution of Eq. (26) may be obtained as a series of time-ordered integrals, i.e.,

$$\hat{\rho}(t,\tau)=\hat{\rho}_0(0,\tau)+\hat{\rho}_1(t,\tau)+\hat{\rho}_2(t,\tau)+\cdots, \quad (27)$$

where $\hat{\rho}_0(0,\tau)=\exp(-i\hat{G}\tau)\hat{\rho}(0)\exp(i\hat{G}\tau)$ and is the density matrix after the initial 90° pulse, but just before the spin-locking field is switched on. The nth term in the expansion is given by

$$\hat{\rho}_n(t,\tau)=(-i)^n\int_0^t dt_1\cdots\int_0^{t_{n-1}}[\hat{G}(t_1),[\cdots,[\hat{G}(t_n),\hat{\rho}(\tau)]\cdots]]_n dt_n. \quad (28)$$

The subscript n and the dots denote an n-fold time-ordered commutation of $\hat{G}(t)$ with $\hat{\rho}(\tau)$.

1. *Evaluation of Transient Response*

We wish to evaluate the spin-locked magnetization at exact resonance, i.e., $\Delta\omega=0$. Thus we require

$$\langle I_z\rangle=\sum_n\langle I_z\rangle_n=\sum_n\mathrm{Tr}\{\hat{\rho}_n(t,\tau)I_z\}. \quad (29)$$

We specialize to $\tau=0$ for simplicity, although this is strictly not equivalent to the multiple-pulse experiment.

In order to introduce damping in Eq. (29) it is necessary to carry the calculation to at least fourth order in the perturbation expansion. Using the commutation relation

$$[I_z,G_M]=MG_M, \quad (30)$$

and the transformation

$$\exp(-i\omega_rI_zt)G_M\exp(i\omega_rI_zt)=G_M\exp(-iM\omega_rt), \quad (31)$$

and noting that the terms for odd n vanish in Eq. (29), we evaluate the even terms as follows.

Zeroth-order term. This case is trivial and corresponds to the free-induction decay amplitude at $\tau=0$, i.e.,

$$\langle I_z\rangle_0=\mathrm{Tr}\{\hat{\rho}_0(0)I_z\}, \quad (32)$$

where $\hat{\rho}_0(0)=aI_z$. We do not include the dipolar part of the density matrix in this treatment. For dipolar-Zeeman cross-relaxation processes, discussed later on, this must be included, together with a two-temperature assumption following the work of Provotorov[25] and of Walstedt.[19] In the present calculation we tenta-

[24] A. G. Redfield, Phys. Rev. **98**, 1787 (1955).

[25] B. N. Provotorov, Zh. Eksperim. i Teor. Fiz. **41**, 1582 (1961) [English transl.: Soviet Phys.—JETP **14**, 1126 (1962)].

tively assume that cross-relaxation is slow compared to the Zeeman temperature equilibration time, which is related to T_2.

Second-order term. From Eqs. (28) and (29) this is

$$\mathrm{Tr}\{\hat{\rho}_2(t)I_z\}$$

$$=a\,\mathrm{Tr}\left\{\int_0^t dt_1\int_0^{t_1} dt_2[\hat{G}(t_1),[\hat{G}(t_2),I_z]]I_z\right\}. \quad (33)$$

Since we are discussing the case at resonance, $\Theta=90°$, therefore

$$\hat{G}(t)=G_0+\exp(-i2\omega_r t)G_2+\exp(i2\omega_r t)G_{-2}, \quad (34)$$

and

$$[\hat{G}(t),I_z]=2\exp(-i2\omega_r t)G_2-2\exp(i2\omega_r t)G_{-2}. \quad (35)$$

Thus rearranging the trace, substituting for the commutators, and integrating, we obtain

$$\langle I_z\rangle_2=8a[(\cos2\omega_r t-1)/(2\omega_r)^2]\,\mathrm{Tr}\{G_2G_{-2}\}, \quad (36)$$

since $\mathrm{Tr}\{G_MG_{M'}\}$ is zero unless $M+M'=0$.

Fourth-order term. Substituting for the commutators, multiplying out, and noting that the only nonvanishing traces occurring are $\mathrm{Tr}\{[G_0,G_2][G_0,G_{-2}]\}$ and $\mathrm{Tr}\{[G_2,G_{-2}]^2\}$, we obtain finally after integration, for the fourth-order contribution,

$$\langle I_z\rangle_4=4a\left[\mathrm{Tr}\{[G_2,G_{-2}]^2\}\left(\frac{-4(\cos2\omega_r-1)}{(2\omega_r)^4}-\frac{2t\sin2\omega_r t}{(2\omega_r)^3}\right)-\mathrm{Tr}\{[G_0,G_2][G_0,G_{-2}]\}\times\left(\frac{6(\cos2\omega_r t-1)}{(2\omega_r)^4}-\frac{t^2\cos2\omega_r t}{(2\omega_r)^2}+\frac{4t\sin2\omega_r t}{(2\omega_r)^3}\right)\right]. \quad (37)$$

Adding all contributions and simplifying the notation we obtain

$$\langle I_z\rangle=b\{1-\Gamma_1+\Gamma_1[(1+4Bt^2/(2\omega_r)^2\Gamma_1)\cos2\omega_r t-2\omega_r t(\Gamma_2/\Gamma_1)\sin2\omega_r t]\}, \quad (38)$$

where

$$\Gamma_1=+8A/(2\omega_r)^2-(24B+16C)/(2\omega_r)^4+\cdots \quad (39a)$$

and

$$\Gamma_2=(16B+8C)/(2\omega_r)^4+\cdots. \quad (39b)$$

The quantities appearing in Eqs. (39a) and (39b) are defined as follows:

$$A=\mathrm{Tr}\{G_2G_{-2}\}/\mathrm{Tr}\{I_z^2\},$$

$$B=\mathrm{Tr}\{[G_0,G_2][G_0,G_{-2}]\}/\mathrm{Tr}\{I_z^2\},$$

$$C=\mathrm{Tr}\{[G_2,G_{-2}]^2\}/\mathrm{Tr}\{I_z^2\},$$

$$b=a\,\mathrm{Tr}\{I_z^2\}.$$

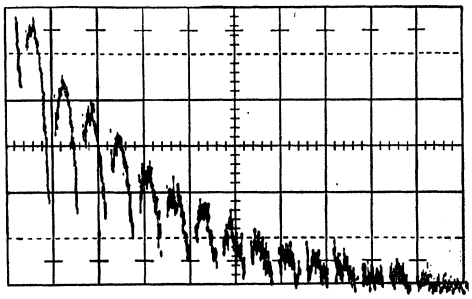

FIG. 3. Photograph of positively detected solid-echo train in a single crystal of CaF_2 with its [111] axis along $\mathbf{H}_0$. The 90° pulses are too fast to be observed. Only the evolution of the magnetization between pulses is observed. $\tau=30$ μsec and the time-base sweep is 100 μsec/div.

2. Gaussian Damping Function Approximation

Contracting the trigonometric expressions in Eq. (38), we obtain the approximate form

$$\langle I_z\rangle\simeq b\{1-\Gamma_1+\Gamma_1(\cos2\omega_r t(1+\Gamma_2/\Gamma_1)+[4Bt^2/(2\omega_r)^2\Gamma_1]\cos2\omega_r t+\cdots)\}. \quad (40)$$

This is valid if

$$2\omega_r\Gamma_2 t/\Gamma_1\ll1. \quad (41)$$

Because we truncated the expansion at $n=4$, Eq. (40) does not exhibit damping as it stands. However, the appearance of the $4Bt^2/(2\omega_r)^2\Gamma_1$ term suggests that it is the first term of a damped function of time. Through a lack of knowledge of the higher-order terms, which would be extremely tedious to calculate, we assume the form of the damping function is Gaussian. In this case, we may write Eq. (40) in approximate, but closed form as

$$\langle I_z\rangle\simeq b\{1-\Gamma_1+\Gamma_1\exp[4Bt^2/(2\omega_r)^2\Gamma_1]\times\cos2\omega_r t(1+\Gamma_2/\Gamma_1)\}. \quad (42)$$

When expanded in powers of time Eq. (42) agrees with the exact expression up to t^2. The inequality Eq. (41) is well satisfied over the range of interest in the experiments presented, i.e., for the spin-locking field greater than the local field. The truncation of Γ_1 and Γ_2 is also justified if we restrict ourselves to high fields.

C. Thermal Equilibrium

The calculation presented in Sec. IIB represents the approach of the spin-locked system to a quasiequilibrium state in a constant rf field. From a classical view, we may regard the initial oscillatory nature of the magnetization as originating from coherent precession of the spins about a distribution of effective fields. In particular, the ith spin situated in its local field will precess about its effective field, which is the vector sum of $\mathbf{H}_r$ and the local field at the spin site. Because of the spin-flip terms, the local field is not static, but changes

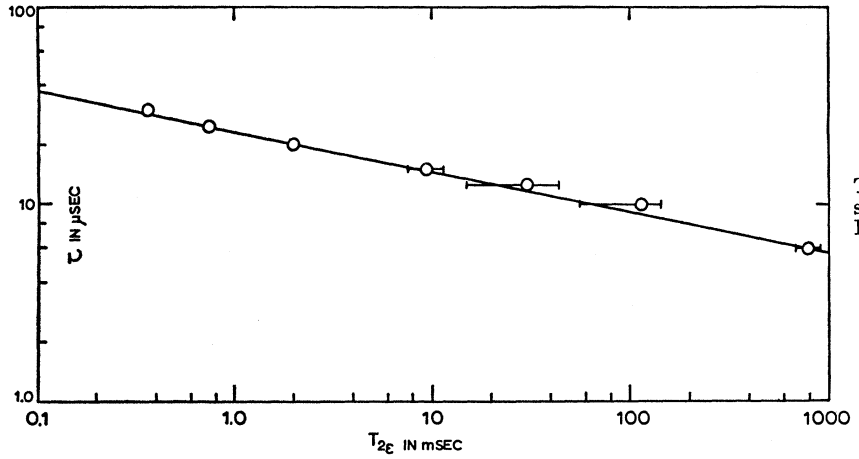

FIG. 4. Log–log graph of $T_{2\epsilon}$ versus τ. The circles are experimental data. The solid line is the theoretical expression, Eq. (20).

classically at angular frequency $\omega_{r\,\mathrm{eff}}$. Thus the z component of magnetization oscillates at $2\omega_{r\,\mathrm{eff}}$. We point out that in a spin system consisting of two magnetic ingredients, and when the local field at the resonant spin site is dominated by the nonresonant spin species, the spin-flip term is quenched. In this case the local field is nearly static, and the transient oscillations occur at angular frequency ω_r.

It is clear from the previous section and other calculations[15,16] that while we have been concerned with evaluating the Zeeman magnetization only, the expectation value of the dipolar Hamiltonian will be nonzero and time-dependent also. Thus the initial oscillations also correspond to a mutual exchange of energy between the Zeeman and dipolar systems. When the oscillations have died out we may describe the Zeeman system by a time-independent density matrix in the rotating frame. That is to say, the quasiequilibrium state is characterized by a spin temperature. This will in general be lower than the initial lattice temperature. We regard the establishment of a Zeeman spin temperature as the first stage in the approach of the system to thermodynamic equilibrium. The second stage is thermal mixing with the dipolar subsystem, therefore establishing a final common spin temperature. The rate at which stage two occurs has been studied theoretically by Provotrov[25] and adapted by Walstedt[19] and is discussed later.

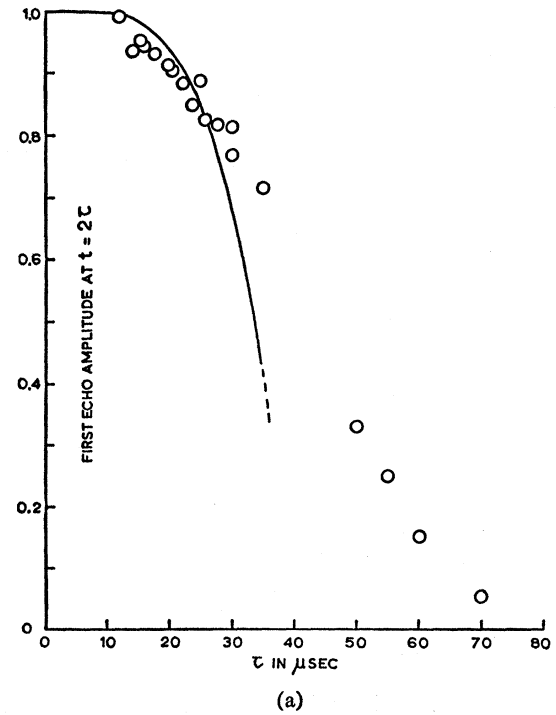

(a)

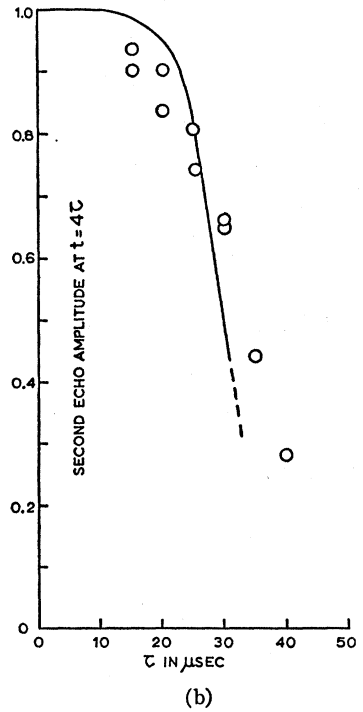

(b)

FIG. 5. Experimental solid-echo amplitudes (circles) in CaF_2 with $\mathbf{H}_0$ along the [111] axis. (a) Normalized first-echo amplitude at $t=2\tau$ versus τ. The solid line is the theoretical expression, Eq. (4). (b) Normalized second-echo amplitude at $t=4\tau$ versus τ. The solid line is the approximate theoretical expression [right-hand side of Eq. (15).]

1. Conservation of Energy

The procedure of rapid spin-locking described previously and represented in Fig. 1(c) corresponds to the sudden approximation in quantum mechanics. Slichter and Holton[26] have discussed this for a similar system involving a single long pulse off resonance.

Immediately following the spin-locking field the magnetic energy of the system is

$$E=-M_0H_r-CH_L^2/T_L, \tag{43}$$

where $M_0=CH_0/T_L$ is the equilibrium magnetization in the static field, and T_L is the initial lattice temperature. H_L is the local field defined by the relation $H_L^2=\mathrm{Tr}\{\rho G\}$ and $C=NI(I+1)\gamma^2\hbar^2/3k$ is Curie's constant. We equate this to the energy of the spin system at equilibrium, i.e.,

$$M_0H_r+CH_L^2/T_L=M_fH_r+CH_L^2/T_f, \tag{44}$$

where the subscript f refers to the final state, and T_f is the final common spin temperature of the dipolar and Zeeman thermal reservoirs. Rearranging Eq. (44) we obtain

$$M_f=M_0\frac{(H_r^2+H_rH_L^2/H_0)}{H_r^2+H_L^2}\simeq\frac{M_0H_r^2}{H_r^2+H_L^2}. \tag{45}$$

It is of interest to compare this expression with the case of adiabatic demagnetization from an initial state i in high field to a lower final state. This gives

$$M_f=M_0\frac{H_r}{H_{ri}}\left(\frac{H_{ri}^2+H_L^2}{H_r^2+H_L^2}\right)^{1/2}\simeq\frac{M_0H_r}{(H_r^2+H_L^2)^{1/2}}$$

for $H_{ri}\gg H_L$. The constant-entropy curve predicts slightly higher final magnetization for given H_r and H_L than the constant-energy curve [Eq. (45)]. The difference in magnetization represents an irreversible loss due to transverse relaxation in the local fields.

2. Dipole-Zeeman Cross Relaxation

The basis for the calculation of the approach to thermal equilibrium has been given by Provotorov, and adapted by Walstedt[19] to the case of large H_r. The calculation is strictly only valid when the nonsecular terms coupling the Zeeman-dipolar terms are small with respect to both of these. In this case, a two-spin temperature assumption seems valid. In our case, with dipolar spin-spin coupling only, the above condition is not satisfied, the nonsecular terms in this case being of the same order as the secular terms.

In view of the quasiequilibrium state, it might be more appropriate to consider a three-temperature system in which the Zeeman and nonsecular dipolar terms form a reservoir at an intermediate spin temperature, which finally cross-relaxes with the secular dipolar reservoir.

[26] C. P. Slichter and W. C. Holton, Phys. Rev. **122**, 1701 (1961).

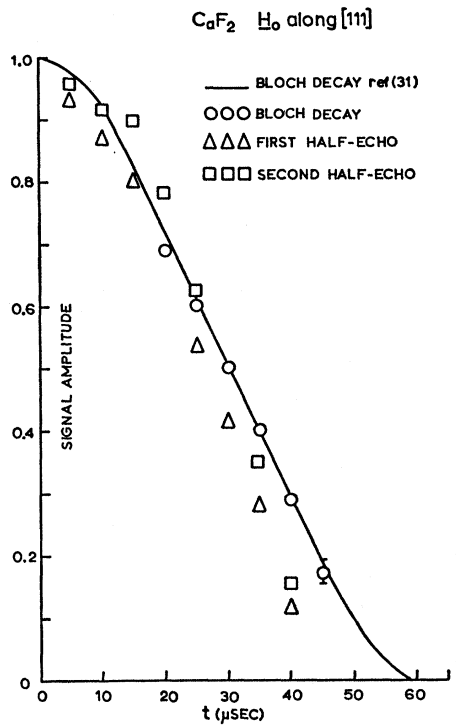

FIG. 6. Comparison of the free induction decay with the first and second echoes for times greater than or equal to 2τ and 4τ, respectively.

We do not propose to pursue this model here, but rather we shall take the two-temperature assumption of Walstedt. It is certainly true that the establishment of the quasiequilibrium state is very rapid. Thus for all practical purposes, the slow cross-relaxation process follows a two-temperature model.

For convenience, we write Walstedt's expression for the Zeeman-dipolar cross relaxation time in our notation as follows:

$$T_{ZD}^{-1}=\sum_M M^2\,\mathrm{Tr}\int_{-\infty}^{\infty}dt\,\exp(iM\omega_r t)\times\{G_M\exp(iG_0t)G_{-M}\exp(-iG_0t)\}/\mathrm{Tr}\{I_z^2\}, \tag{46}$$

where $M=1$, 2. Also making the assumption of a Gaussian distribution of local fields, the trace simplifies to

$$\mathrm{Tr}\{G_M\exp(iG_0t)G_{-M}\exp(-iG_0t)\}\simeq\mathrm{Tr}\{G_MG_{-M}\}\times\exp(-t^2/a_M^2), \tag{47}$$

where

$$1/a_M^2=-\tfrac{1}{2}\mathrm{Tr}\{[G_0,G_M][G_0,G_{-M}]\}/\mathrm{Tr}\{G_MG_{-M}\}.$$

In our case, $M=2$ only since we are presently interested in cross relaxation at exact resonance. Thus integrating Eq. (46) we find that

$$1/T_{ZD}=4A(-2A\pi/B)^{1/2}\exp(2A\omega_r^2/B), \tag{48}$$

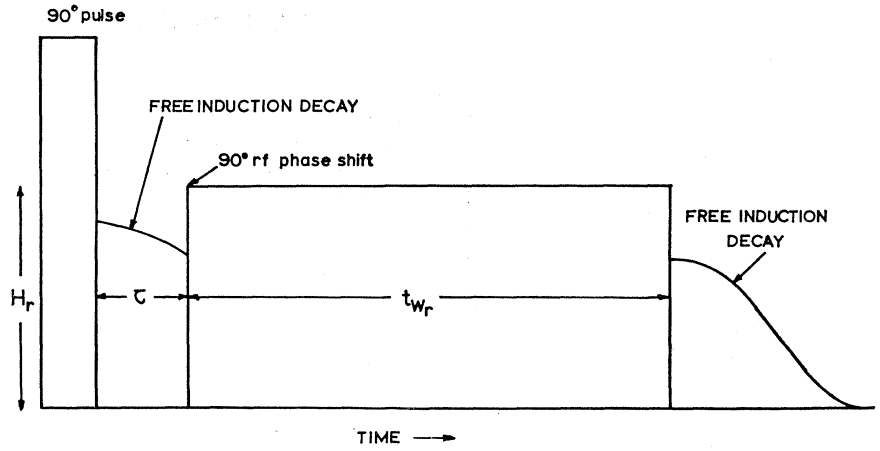

FIG. 7. Sketch of pulse sequence used in the long-pulse spin-locking experiments.

where A and B are as defined previously in Sec. IIB. We notice that within the assumptions made in Walstedt's calculation, the cross-relaxation process involves fewer lattice sums than the similar calculation for establishment of the Zeeman spin temperature. Implicit in Eq. (48) is the two-temperature density-matrix assumption and single exponential relaxation. We note from Eq. (48) that for $\omega_r=0$, $T_{ZD}\simeq T_2$. As expected, T_{ZD} rapidly increases for large ω_r. This corresponds to the decreased ability of the dipole system to conserve the energy of the Zeeman transitions. For ω_r large, T_{ZD} is rather sensitive to the spectral distribution of the dipole reservoir, particularly in the wings. This makes T_{ZD} especially sensitive to the form of the spectral assumption made.

III. EXPERIMENTAL DETAILS AND RESULTS

A. Apparatus

The multiple-pulse sequences are produced with a coherent high-power transmitter. The signal from a freely running 9.0 Mc/sec crystal oscillator is fed to two Blume gates[27] via two resistance-capacitance phase shifters. The gate outputs are combined and amplified in a broad-band amplifier to produce a linear rf magnetic field at the sample of 100 G, corresponding to a 90° pulse length of 1.3 μsec for fluorine spins. The circuits are of straightforward design. The receiver is a broad-band synchronously tuned amplifier[28] but modified to take a reference signal for coherent detection. The recovery time measured from the end of the gating pulse is 10 μsec. In the long-pulse experiments, because of the necessity of varying H_r, an entirely separate gated amplifier[29] is used. The input of this amplifier is fed from the reference signal. The output is directly combined with the short-pulse amplifier output at the transmitter head matching circuit. In this way, it is possible to produce a short high-power 90° pulse followed by a phase-shifted long low-power pulse.

The signals were either photographically recorded directly from an oscilloscope trace, or recorded using a digital 'boxcar' circuit[30] developed in this laboratory. A Varian 9-in. field-stabilized electromagnet provided the static field. The calcium fluoride crystals were obtained from Harshaw Chemicals Inc., and all data were recorded at a temperature of 298°K. The crystal was aligned with $\mathbf{H}_0$ along the [111] direction by observing the maximum time to the first-free induction decay zero and judged to be correct to better than 1°, in agreement with the experiments of Barnaal and Lowe.[31] With this orientation $T_2\simeq 30$ μsec and $T_1\simeq 6.0$ sec.

The transmitter coil is a rectangular cylindrical Helmholtz construction following the design of Lurie and Slichter.[13] The receiver coil is fixed with its axis orthogonal to the transmitter coil, but allowing easy removal and orientation of the sample.

B. Multiple Solid-Echo Trains

Multiple-pulse $90°-\tau-90°_{90°}-[2\tau-90°_{90°}]_{N-1}$ sequences have been applied at the Larmor frequency to the F^{19} spins in CaF_2. The effect of these pulses is to prolong the free induction decay by many orders of magnitude. This is equivalent to artificially narrowing the resonance absorption line shape. The amplitudes of successive multiple echoes were mostly found to decay exponentially. There is a very small oscillation of the first few echoes, however, but in a single-species spin system this is of the same order as the noise and is hard to detect. For $\tau\sim T_2$, well-resolved echoes are obtained (Fig. 3), but for close pulse spacing, the individual echoes merge into an apparently continuous signal. In this case, for $\tau<10$ μsec we have observed non-exponential monotonic behavior, but we attribute this to receiver recovery. The best exponential fit was taken in these cases, giving rise in some instances to rather large errors. Since the receiver-recovery effects tend to

[27] R. J. Blume, Rev. Sci. Instr. **32**, 554 (1961).
[28] P. Mansfield and J. G. Powles, J. Sci. Instr. **40**, 232 (1963).
[29] We are indebted to Mr. D. K. Needham for constructing the long-pulse transmitter.
[30] D. Ware and P. Mansfield, Rev. Sci. Instr. **37**, 1167 (1966).
[31] D. E. Barnaal and I. J. Lowe, Phys. Rev. **148**, 328 (1966).

increase the observed T_{2e}, we would attach more weight to the short end of the error bar. The experimental results together with the theoretical expression Eq. (20) are plotted in Fig. 4. Variation of the phase shift by $\pm 20°$ about the 90° condition made no appreciable difference to the observed values of T_{2e}. We have also measured the first-echo amplitude at $t=2\tau$ and the second-echo amplitude $t=4\tau$ for various pulse spacings. These results are plotted in Figs. 5(a) and (b) together with the theoretical expressions, Eq. (4), and the right-hand side of Eq. (15). Since the coefficient of τ^4 vanishes for the second echo, we might expect the second solid half-echo shape to be closer to the initial free induction decay shape than the first solid half-echo. Experimental data in Fig. 6 confirms this and is also compared with Barnaal and Lowe's free induction decay.[31] Checks out to the first fourteen echoes indicate that odd echoes are narrower than even echoes. This supports our assumption regarding the diagonality of the density matrix.

C. Long-Pulse Spin-Locking Experiments

Experiments have been performed on fluorine in CaF_2 at exact resonance in which the magnetization following an initial 90° rf pulse is rapidly spin locked at time τ later in a second long, low-power rotating magnetic field H_r of pulse length t_{wr}. This is achieved by a 90° rf phase shift of the long pulse. The state of the spin system is observed by rapidly switching off the spin-locking field and observing the amplitude of the free induction decay. The pulse sequence is illustrated in Fig. 7. All data is taken with $\mathbf{H}_0$ along the [111] direction.

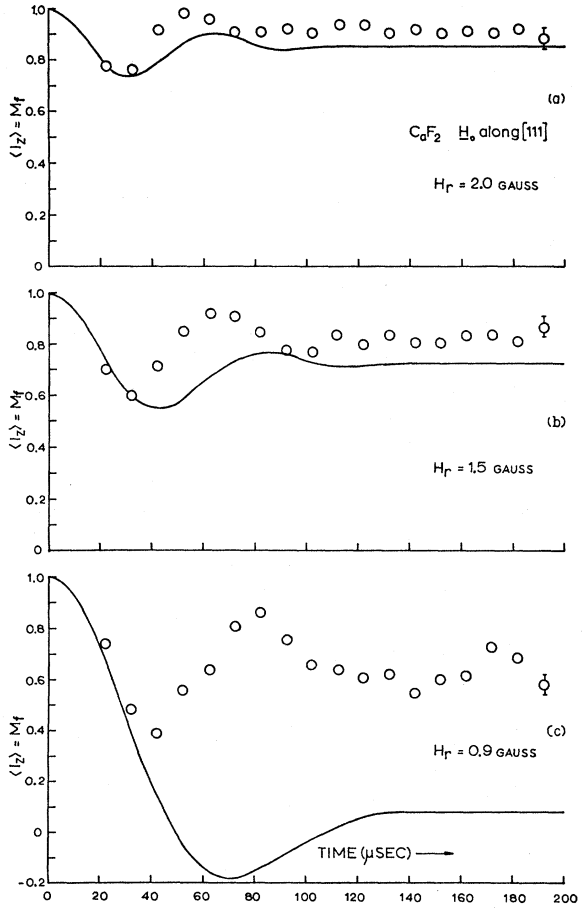

FIG. 8. Spin-locked magnetization versus t_{wr} for various spin-locking fields H_r, together with the theoretical expression, Eq. (42).

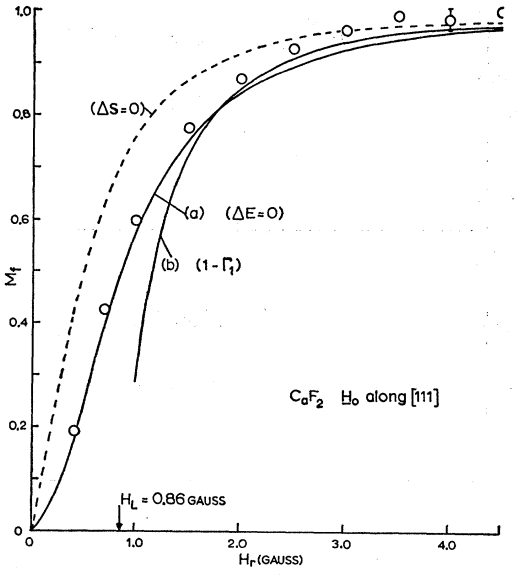

FIG. 9. Spin-locked magnetization versus magnetic field H_r for t_{wr} fixed at 10 msec. The solid curve (a) is the theoretical final thermal equilibrium value as given by Eq. (45). Curve (b) is the theoretical quasiequilibrium time-independent part of Eq. (42). The dotted curve corresponds to an adiabatic demagnetization from an initially high field.

For fixed H_r, the spin-locked magnetization is found to oscillate as a function of t_{wr} damping out to a quasi-equilibrium value in around 100 μsec. We have repeated these experiments for a number of values of spin-locking field. Results for $H_r=2.0$, 1.5, and 0.9 G are shown in Fig. 8, together with the theoretical expression, Eq. (42). We note in Fig. 8(a) that reasonable agreement between theory and experiment is obtained. For lower fields, the oscillations become more violent, Fig. 8(b) and 8(c). Unfortunately, the theory rapidly breaks down here due to the truncation of Γ_1 and Γ_2 at fourth order. The disappearance of the oscillations corresponds to an establishment of a Zeeman spin temperature. We have plotted the experimental spin-locked magnetization out to $t_{wr}=10$ msec and for $H_r=$ 2.0 and 1.5 G there is a further small monotonic decrease in amplitude of the equilibrium magnetization. We attribute this to dipole-Zeeman cross relaxation and this is discussed separately. Although we give no theoretical analysis for nonzero τ, in these experiments, we find that provided the time origin is taken immediately following the 90° pulse, the high-field data seem to fit Eq. (42) independent of τ at least up to 10 μsec.

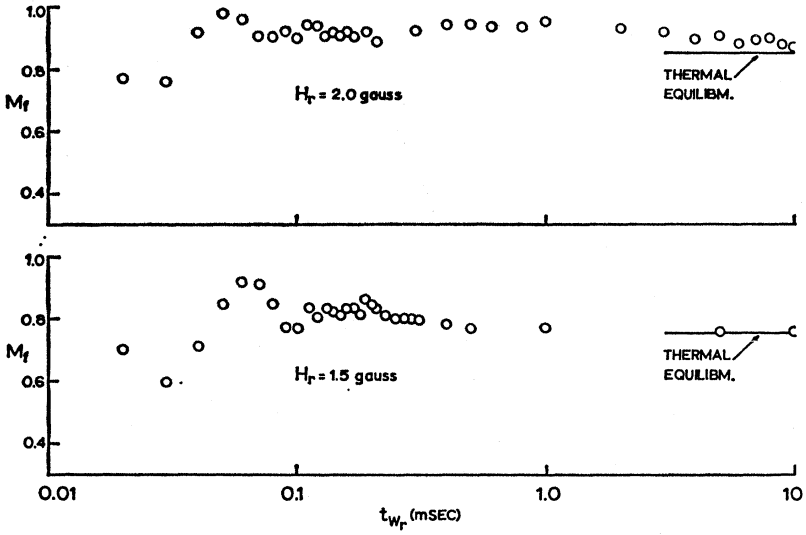

FIG. 10. Semilogarithmic plot of curves (a) and (b) in Fig. 8 out to $t_{wr}=10$ msec. The experimental points indicate a departure from the quasiequilibrium value, slowly approaching the thermal equilibrium magnetization.

D. Equilibrium Magnetization

Long-pulse spin-locking experiments were performed with t_{wr} held at 10 msec and with H_r varied from 0.5 up to 6.0 G. The experimental data are plotted in Fig. 9. These are compared with the theoretical curve [Eq. (45)], which assumes that the initial magnetic energy is conserved and that the dipole and Zeeman energy reservoirs equilibrate to a common spin temperature. In CaF_2 for $\mathbf{H}_0$ along the [111] axis, the local field $H_L=0.86$ G. We see that good agreement is obtained between theory, [solid curve (a), Fig. 9] and the data for $H_r<H_L$. For increased H_r, the magnetization does not come into equilibrium with the dipolar reservoir in the time of the experiment. The normalized magnetization in this case is predicted by the time-independent part of Eq. (42), i.e., $\langle I_z\rangle=1-\Gamma_1$. This expression is also plotted, [curve (b), Fig. 9]. We see there is good experimental agreement for high field. As expected, however, the theoretical expression breaks down for $H_r\leq 2H_L$, as indicated by the sharp downwards deviation at $H_r\simeq 1.75$ G.

As a matter of comparison, we also plot in Fig. 9 the theoretical magnetization for a sample which is adiabatically demagnetized from an initial field much greater than H_L. The quasiequilibrium state clearly should always fall between the two extreme curves of constant entropy and constant energy.

The experimental data of Figs. 8(a) and 8(b) is replotted semilogarithmically in Fig. 10 to include all points out to 10 msec. This illustrates the slow cross relaxation between the dipolar and Zeeman reservoirs. For $H_r=1.5$ G the data indicate exponential cross relaxation with a time constant $T_{ZD}=0.37$ msec. Since all the data of Fig. 9 is taken with $t_{wr}=10$ msec, we can infer a lower limit for T_{ZD} for $H_r>2.0$ G. Our experimental values of T_{ZD} are plotted in Fig. 11 together with the theoretical expression, Eq. (48). We see that there is order-of-magnitude agreement. Since Eq. (48) is critically dependent on the Gaussian assumption for the dipolar spectral distribution, the agreement is gratifying. The exact form of the spectral distribution can be obtained experimentally from the damping of the initial oscillations and used to calculate the cross-relaxation time. However, since the Gaussian approximation is so good for large H_r, it is doubtful if much better agreement with the cross-relaxation data would result. We stress here that some of the difference between theory and experiment is doubtless ascribable to the large uncertainty in the data.

In order to improve the dipolar spectral distribution function, Eq. (38) would need to be carried through to at least sixth order.

IV. CONCLUSIONS

We have shown experimentally that for the F^{19} resonance in a single crystal of CaF_2, the free induction decay following a 90° rf pulse can be prolonged many orders of magnitude by further application at time τ of a coherent train of 90° pulses uniformly spaced at 2τ. The rf phase of the pulse train is shifted 90° with respect to the initial pulse. The effect of these pulses is to produce a continuous train of solid echoes. This corresponds to a narrowing of the resonance absorption line shape plus the introduction of side bands, and is most effective for $\tau<T_2$. The evolution of the spin magnetization is observed between the rf pulses and the peaks of successive solid echoes are found to decay exponentially with an effective relaxation time T_{2e} which is a function of τ. Measurements of T_{2e} versus τ have been made and for the shortest τ used (around 6 μsec), the transverse decay persists for as long as 1.0 sec. The normal transverse relaxation time $T_2\sim 30$ μsec for $\mathbf{H}_0$ along the [111] direction.

A theoretical expression is derived relating T_{2e} and τ, and is based on a diagonal assumption for the density matrix describing the even-echo peaks. This gives the

correct τ dependence. Evaluation of the magnitude of $T_{2\epsilon}$ using an approximate trace calculation gives remarkably good agreement with experiment. In these calculations, spin-lattice-relaxation effects are entirely ignored.

Calculations of the first three echoes shows that there should be a small oscillation of amplitude, the second echo being slightly higher than the first. The diagonal assumption carries this oscillation throughout the echo train, but with reduced amplitude. Since the effect is so small, we have not been able to definitely resolve it experimentally. In spin systems composed of two magnetic ingredients, and where the nonresonant spin contribution to the second moment is large, we would expect a much larger oscillating effect. Also, because of the different rotational symmetry of the I-S term in the dipolar Hamiltonian, the period should be twice as long. A full discussion of this case will be given later.

The continuous rf pulse train can be represented by an even Fourier series composed of a mean cw rf field plus cosine modulated harmonics of the pulse period. For very close pulse spacing, the pulse train becomes more like a cw signal. In the limit, when the pulses merge, we have the normal spin-locked condition.

The physical nature and origin of the solid-echo amplitude modulation may be understood by simulating the rf pulse train. This has been done by applying at resonance a long continuous spin-locking pulse of low power immediately following the initial 90° pulse. Large damped oscillations of the longitudinal or spin-locked magnetization about a final steady value have been observed for several values of the spin-locking field. The oscillations are due to coherent precession in a distribution of effective fields. Theoretical expressions based on a perturbation expansion of the density matrix are given which predict the correct periodicity and final steady value of the magnetization. Dissappearance of the oscillations corresponds to the establishment of a spin temperature in the Zeeman energy reservoir. For $H_r<2H_L$ the perturbation expansion breaks down. The final magnetization may be calculated in this region by assuming that the initial spin-locked magnetic energy is conserved. In this case, a redistribution of energy between the Zeeman and dipole energy reservoirs takes place fairly rapidly, thereby establishing a common spin temperature in the system. This is a good approximation when the dipolar spectral width is comparable to the Zeeman splitting, i.e., when $H_r<H_L$. Experimental results give good agreement with the theory. For $H_r>H_L$, the establishment of a common spin temperature takes longer, due to slower cross relaxation. For $H_r>2.0$ G, the experimental results indicate that very little redistribution of magnetic energy has taken place in 10 msec. Thus, we are able to infer a lower limit to the cross-relaxation time T_{ZD}. We have also estimated a value for an intermediate field of 1.5 G. Our values agree within an order of magnitude with those predicted by Walstedt. His theory uses a similar Gaussian assumption for the dipolar spectral distribution as we make here for the damping of the initial oscillations. Since we find good agreement in the transient experiments with the Gaussian damping approximation for high fields, the exact form for the dipolar spectral distribution, obtained experimentally, would probably not improve agreement with our cross-relaxation data. In view of the rather large errors in T_{ZD}, due to the relatively small reduction in magnetization involved in achieving final thermal equilibrium, it would be surprising to obtain quantitative agreement with the cross-relaxation theory.

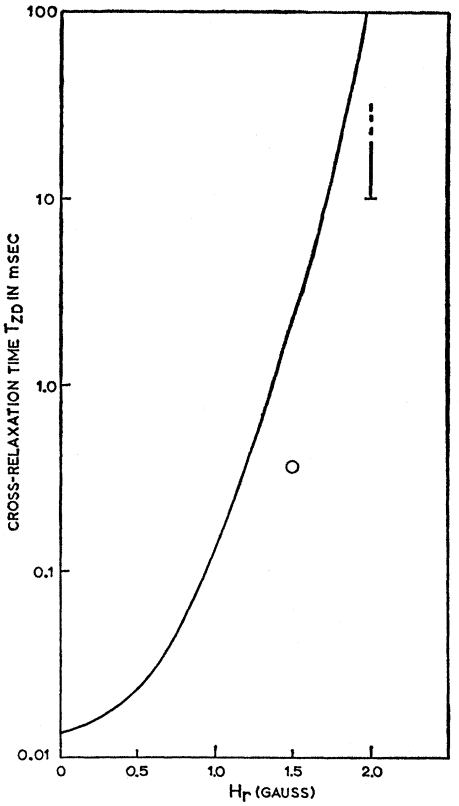

FIG. 11. Theoretical Zeeman dipolar cross relaxation time T_{ZD} versus H_r. Also plotted is one experimental point estimated from Fig. 10(b) and a lower limit estimated from Fig. 9.

APPENDIX A: MULTIVARIANT CUMULANT EXPANSION

In this Appendix, we define the multivariant cumulant averages or connected averages, and relate them to the normal Van Vleck moments of the absorption line shape. The method closely follows that of Horwitz and Callen.[23] For this purpose it is convenient to first consider the transverse response function of a spin system[32] for $t>0$, i.e.,

$$\langle I_x\rangle = \mathrm{Tr}\{\rho(0)[I_+(t), I_-]\} = \langle [I_+(t), I_-]\rangle, \quad \text{(A1)}$$

[32] See, for example, P. Mansfield, Phys. Rev. **151**, 199 (1966).

TABLE I. Lattice sums in inverse angstrom units for CaF_2 with the static field along the principal crystal axes. The first column includes an integrated contribution taken from the 21st shell.[a]

	$\sum_j A_{jk}^2$ (Å^{-6})	$\sum_j A_{jk}^4$ (Å^{-12})	$\sum_{j\neq k} A_{jk}^2 A_{jl} A_{kl}$ (Å^{-12})
[100]	3.259×10^{-2}	2.147×10^{-4}	9.45×10^{-5}
[110]	1.235×10^{-2}	1.664×10^{-5}	2.53×10^{-5}
[111]	5.607×10^{-3}	1.399×10^{-6}	4.12×10^{-6}

[a] *Footnote added in proof.* The values computed here refer to the spatial and angular sums only, i.e., the $2P_2(\cos\theta_{ij})/r_{ij}^3$ part of A_{ij}, etc.

where the angled brackets denote the high-temperature-approximation thermal averages with respect to the unperturbed density matrix and

$$I_+(t)=\exp(i\mathcal{H}_1 t)I_+\exp(-i\mathcal{H}_1 t), \tag{A2}$$

also $I_\pm$ are the usual spin displacement operators.

Introducing the Liouville operator L [see Eq. (14a)] we may write the normalized transverse response function Eq. (A1) as

$$\langle I_x\rangle=\langle[\exp(iLt)I_+, I_-]\rangle/\langle[I_+, I_-]\rangle, \tag{A3}$$

remembering that L operates on everything to the right up to and including I_+.

We now generalize Eq. (A3) for a set of operators L_n, i.e.,

$$\langle[\exp(i\sum_n L_n t_n)I_+, I_-]\rangle/\langle[I_+, I_-]\rangle$$

$$\equiv\exp\Big(\sum_{p_n} K(L_1^{p_1}\cdots L_n^{p_n})\prod_n\frac{(it_n)^{p_n}}{p_n!}\Big), \tag{A4}$$

where n and p_n are positive integers, and p_n runs from 0 to ∞ for all n. Equation (A4) thus defines the set of cumulant averages $K(L_1\cdots L_n)$. This technique is really only applicable to cases involving no logarithmic singularity for finite times. That is to say, it will be particularly useful for line shapes near to Gaussian, as in the case of CaF_2 with the [111] axis along $\mathbf{H}_0$.

In general the Liouville operators are q-numbers. Following Kubo[33] we introduce a symmetrizing operator S such that

$$S(L_1^{p_1}\cdots L_n^{p_n})=\frac{p_1!\cdots p_n!}{(p_1+\cdots p_n)!}\sum_{\mathcal{P}_n}\mathcal{P}_n(L_1^{p_1}\cdots L_n^{p_n}),$$

where $\mathcal{P}$ means that we must take all permutations of the product. The purpose of this operator is to generalize the exponential function so that we may use normal commuting algebra, i.e.,

$$\exp(i\sum_n L_n t_n)\equiv S\prod_n\exp(iL_n t_n). \tag{A5}$$

Thus, provided we take the symmetrized sums as defined above, the usual rules of manipulation of exponential functions apply.

We next introduce a set of vanishingly small c-numbers α_n, and an operator $D_{\alpha_n}=\partial/\partial\alpha_n$, such that

$$\frac{t_n^m D_{\alpha_n}^m}{m!}\left(\frac{\alpha_n^m L_n}{m!}\right)=\frac{t_n^m L_n}{m!}; \tag{A6}$$

i.e., α_n is replaced by t_n. Here m is a positive integer. Thus by applying Eqs. (A6) and (A5) to Eq. (A4) we have

$$\ln\langle[\exp(i\sum_n L_n t_n)I_+, I_-]\rangle$$

$$=\lim_{\alpha\to0}\exp(\sum_n t_n D_{\alpha_n})\ln\langle[S\exp(i\sum_n\alpha_n L_n)I_+, I_-]\rangle. \tag{A7}$$

The notation for the limiting procedure means that we take the limit $\alpha_1\to0$ after all the operations by D_{α_1} are complete, then the limit $\alpha_2\to0$, etc.

We now expand $\exp(\sum_n t_n D_{\alpha_n})$ in a power series and obtain, by substituting Eq. (A7) into the logarithm of Eq. (A4),

$$\sum_{p_n} K(L_1^{p_1}\cdots L_n^{p_n})\prod_n\frac{(it_n)^{p_n}}{p_n!}$$

$$=\lim_{\alpha\to0}\prod_n\sum_{p_n}\frac{(t_n D_{\alpha_n})^{p_n}}{p_n!}\ln\langle[S\exp(i\sum_n\alpha_n L_n)I_+, I_-]\rangle, \tag{A8}$$

where $n\geq1$. The $n=0$ term on the right-hand side of Eq. (A8) is subtracted in the limit $\alpha_1\cdots\alpha_n\to0$ by the normalizing denominator [see Eq. (A4)]. Thus rearranging Eq. (A8) and equating coefficients we obtain for the multivariant cumulants, up to nth order,

$$i^n K(L_1^{p_1}\cdots L_n^{p_n})=\lim_{\alpha\to0}\prod_n D_{\alpha_n}^{p_n}$$

$$\times\ln\langle[S\exp(i\sum_n\alpha_n L_n)I_+, I_-]\rangle, \tag{A9}$$

where $\sum_n p_n=n$. The above expression may be simplified by using the following identity:

$$\lim_{\alpha_1\to0} D_{\alpha_1}\ln\langle[S\exp(i\sum_n\alpha_n L_n)I_+, I_-]\rangle$$

$$=\frac{\langle[SL_1\exp(i\sum_2^n\alpha_n L_n)I_+, I_-]\rangle}{\langle[S\exp(i\sum_2^n\alpha_n L_n)I_+, I_-]\rangle}$$

$$\equiv\langle SL_1\rangle_\alpha. \tag{A10}$$

From Eqs. (A9) and (A10) we may write the cumulant

[33] R. Kubo, J. Phys. Soc. Japan **17**, 1100 (1962).

generating function conveniently as

$$D_{\alpha_n}\langle SL_1\cdots L_{n-1}\rangle_\alpha=\langle SL_1\cdots L_n\rangle_\alpha - \langle SL_n\rangle_\alpha\langle SL_1\cdots L_{n-1}\rangle_\alpha. \quad \text{(A11)}$$

Using Eqs. (A10) and (A11) we generate the first few cumulants as follows:

$$K(L_1)=\langle SL_1\rangle_\alpha, \quad \text{(A12a)}$$

$$K(L_1, L_2)=\langle SL_1L_2\rangle_\alpha-\langle SL_1\rangle_\alpha\langle SL_2\rangle_\alpha, \quad \text{(A12b)}$$

$$K(L_1, L_2, L_3)=\langle SL_1L_2L_3\rangle_\alpha-\langle SL_1\rangle_\alpha\langle SL_2L_3\rangle_\alpha - \langle SL_2\rangle_\alpha\langle SL_1L_3\rangle_\alpha - \langle SL_3\rangle_\alpha\langle SL_1L_2\rangle_\alpha + 2\langle SL_1\rangle_\alpha\langle SL_2\rangle_\alpha\langle SL_3\rangle_\alpha. \quad \text{(A12c)}$$

For the special case of the response function [Eq. (A1)] the Liouville operators are all identical and therefore commute. The symmetrizing operator may therefore be replaced by unity. In this case by examining the traces we identify

$$\lim_{\alpha\to 0}\langle L^n\rangle_\alpha=\langle L^n\rangle=M_n; \quad \text{(A13)}$$

i.e., the nth Van Vleck moment of the absorption line shape. For complex pulse sequences, the Liouville operators are not in general equal. Averages like $\langle SL_1\cdots L_n\rangle_\alpha$ are not recognizable as normal moments, but are related quantities. For experiments involving repeated 90° pulses, the averages involve only two types of Liouville operator L and L'. Thus we recognize the average $\langle L^2L'^2\rangle$ as the fourth-moment-like term M_{4x} defined previously.

The symmetrized averages are not in general equal to the averages for $S=1$. As an example

$$\langle SLL'L\rangle=\tfrac{1}{3}(\langle LL'L\rangle+\langle L^2L'\rangle+\langle L'L^2\rangle).$$

The last two terms may be reordered by introducing a commutator $C=[\mathcal{H}_1, \mathcal{H}_1']$. In this case

$$\langle L^2L'\rangle=\langle LL'L\rangle+\langle LC\rangle$$

and

$$\langle L'L^2\rangle=\langle LL'L\rangle-\langle CL\rangle,$$

where

$$\langle LC\rangle=\langle[[\mathcal{H}_1, [C, I_+]], I_-]\rangle,$$

and

$$\langle CL\rangle=\langle[[C, [\mathcal{H}_1, I_+]], I_-]\rangle.$$

Substituting these averages we obtain for the symmetrized average

$$\langle SLL'L\rangle=\langle LL'L\rangle+\tfrac{1}{3}(\langle LC\rangle-\langle CL\rangle).$$

All the mixed symmetrized averages can be rearranged in this way by the introduction of further commutation operations. The terms involving C are in the nature of correction terms which in the present work we neglect entirely.

TABLE II. Computed values of quantities defined in Sec. II.

Quantity evaluated along [111]	
M_2	$14.24\pi^2\times10^7$ rad^2 sec^{-2}
M_{4x}	-15.46×10^{17} rad^4 sec^{-4}
A	$17.80\pi^2\times10^6$ rad^2 sec^{-2}
B	$-1.01\pi^4\times10^{15}$ rad^4 sec^{-4}
C	$8.72\pi^4\times10^{14}$ rad^4 sec^{-4}

APPENDIX B: EVALUATION OF TRACE PRODUCTS AND LATTICE SUMS

In this Appendix, we evaluate the various traces occurring in Sec. II. Term A is straightforward to evaluate and is given below. Term B involves the product of two commutators. These may be written

$$[G_0, G_{\pm2}]=\sum_{k>j}(jk)_\pm+(kj)_\pm+\sum_{k>j>l}(jkl)_\pm + (klj)_\pm+(ljk)_\pm,$$

where

$$(jk)_\pm=\pm A_{jk}'D_{jk}'(-I_{\pm j}^2I_{zk}) + (A_{jk}'+B_{jk}')D_{jk}'(I_{\pm j}I_{\pm k}I_{zk}+I_{\pm j}I_{\pm k}/2)$$

and

$$(jkl)_\pm=\pm I_{zj}I_{\pm k}I_{\pm l}\{A_{jk}'(D_{lk}'-D_{lj}') + A_{jl}'(D_{kl}'-D_{kj}')+(B_{jk}'+B_{jl}')D_{kl}'\}.$$

The commutator occurring in term C may be expressed as

$$[G_2, G_{-2}]=\sum_{k>j}(jk)'+(kj)' + \sum_{k>j>l}(jkl)'+(klj)'+(ljk)',$$

where in this case

$$(jk)'=\tfrac{1}{8}B_{jk}'^2(I_{zj}I_{zk}+I_{zj}I_{-k}I_{+k})$$

and

$$(jkl)'=\tfrac{1}{8}(B_{jk}'B_{lj}')I_{zj}(I_{+k}I_{-l}+I_{-k}I_{+l}).$$

The appropriate commutators are multiplied together and summed over all subscripts.

The traces of the spin products are evaluated in the spherical basis using the well-known trace relations.[34]

[34] E. Ambler, J. C. Eisenstein, and J. F. Schooley, J. Math. Phys. **3**, 760 (1962).

All the sums are evaluated for the case when $\Theta=90°$ and $\tilde{A}_{jk}=0$. After much algebra, we obtain the results

$$A=\mathrm{Tr}\{G_2G_{-2}\}/\mathrm{Tr}\{I_z^2\}$$
$$=(3/8N)\sum_{j\neq k}A_{jk}^2I(I+1),$$
$$B=\mathrm{Tr}\{[G_0,G_2][G_0,G_{-2}]\}/\mathrm{Tr}\{I_z^2\}$$
$$=-(9/32N)\sum_{k\neq j}A_{jk}^4[(12I(I+1)+1)/15-\tfrac{2}{3}]$$
$$-(9/24N)\sum_{l\neq k\neq j}(A_{kl}^2A_{jk}^2+2A_{jk}^2A_{jl}A_{kl})I^2(I+1)^2,$$
$$C=\mathrm{Tr}\{[G_2,G_{-2}]^2\}/\mathrm{Tr}\{I_z^2\}$$
$$=(27/64N)\sum_{k\neq j}A_{jk}^4\{4(2I^2+2I+1)/5-1\}I(I+1)$$
$$+(9/24N)\sum_{l\neq k\neq j}A_{jk}^2A_{kl}^2I^2(I+1)^2.$$

The lattice sums required to obtain numerical evaluation have been calculated on an electronic computer (KDF9) for the static magnetic field along the three principal axes in a single crystal of CaF_2. The lattice constant used in these sums is $a=2.7255$ Å, and the sums include all interactions out to 484 nearest neighbors. This corresponds to 21 nearest-neighbor shells, or to a distance of 13.35 Å. The contribution to the single summations from the remainder of the lattice is estimated by an isotropic integration. In the sums involving A_{jk}^2 the integrated contribution is less than 1.0%, whereas in the sums involving A_{jk}^4 the contribution is found to be less than 0.005%. In the $A_{jk}^2A_{jl}A_{kl}$ sum an integrated contribution cannot easily be obtained, but from the convergence of the sum, we estimate the asymptotic value to differ from our truncated value by less than 10%. The lattice sums required to evaluate all quantities in this paper are presented in Table I. Using these results, the numerical values of the quantities appearing in Sec. II have been calculated and are given in Table II.

PHYSICAL REVIEW VOLUME 168, NUMBER 2 10 APRIL 1968

Isotope Effect in Crystal-Field Splitting

CHAO-YUAN HUANG
Department of Physics and Condensed State Center, Case Western Reserve University, Cleveland, Ohio
(Received 14 September 1967)

The Van Vleck orbit-lattice interaction attributed to the normal coordinates of the cubic molecular cluster transforming like Γ_{4u} is used to calculate the ground-state splitting induced by the lattice vibrations. With the aid of the result obtained by Visscher, we have shown that the isotope shift in the crystal field splitting of the ground state follows the isotope-mass-difference-ratio relationship. We have also found that the temperature-dependent part of the isotope shift is due to the quantum corrections and should vanish in the classical limit.

THE isotope effect in the crystal-field splittings for the ground states of Fe^{3+} in calcite, Cr^{3+} in magnesium oxide and Gd^{3+} in thorium oxide have been observed by Marshall and his co-workers.[1–3] According to their experimental data and analyses, the isotope shifts in the ground-state splittings follow a simple isotope-mass-difference-ratio relationship. They were able to interpret their results by proposing a mechanism in which they included the influence of the dynamical crystal field. In this mechanism, they assumed that the molecular cluster is completely isolated from the rest of the crystal and that the frequency of vibrations of this complex is given by a simple relation $\omega_c=(K/M')^{1/2}$, where M' was regarded as the mass of the paramagnetic ion. In a real crystal, it is not easy to justify this isolated complex model because, as specifically pointed out by Van Vleck,[4] the vibrations of the ions in a molecular cluster arise from the lattice vibrations of the crystal as a whole. Furthermore, the relation between the frequency of the vibration of the complex and the mass of the paramagnetic ion is not so simple.[5] In this paper, we shall use the Van Vleck orbit-lattice interaction and shall try to interpret the isotope effect in the crystal-field splitting of the ground state in a more natural way. However, for simplicity, we shall restrict ourselves to the XY_8 cubic molecular cluster and also focus our attention to the discussion of the isotope effect in Gd^{3+} doped thorium oxide in which Gd^{3+} sits at the center of the XY_8 cubic molecular cluster with eight oxygen ions at the corners.

[1] S. A. Marshall, J. A. Hodges, and R. A. Serway, Phys. Rev. **133**, A1427 (1964).
[2] S. A. Marshall, J. A. Hodges, and R. A. Serway, Phys. Rev. **136**, A1024 (1964).
[3] S. A. Marshall, Phys. Rev. **159**, 191 (1967).
[4] J. H. Van Vleck, Phys. Rev. **57**, 426 (1940).
[5] The relation, $\omega=(K/M')^{1/2}$, is not true even for the XY_2 molecular cluster [see, for example, Gerhard Herzberg, *Molecular Spectra and Molecular Spectra* (D. Van Nostrand Company, Inc., Princeton, N.J., 1954), p. 154].